

Texas Instruments Innovation Challenge: Europe Analog Design Contest 2014
Project Report

Tlagnose Watch

Team Leader:	Stijn Wielandt - stijn.wielandt@kuleuven.be
Team Members:	Steven De Lausnay - steven.delausnay@kuleuven.be
Advising Professor:	Nobby Stevens - nobby.stevens@kuleuven.be
University:	KU Leuven - Belgium
Date:	[31.07.14]

Qty.	TI Part Number & URL	Qty.	TI Part Number & URL
1	BQ51013B	1	LMV344
1	BQ24640	1	MSP430FR5969
1	TLV61220	8	CSD13202Q2
1	LP2981-33	1	CC110L – Anaren A110LR09A
1	TLV71310p	1	TMP006
1	BQ500210EVM	1	MSP-EXP430G2
1	430BOOST-CC110L		



Project abstract: A wristband device was developed for use by medical staff in maternity hospitals. The device performs measurements of the body temperature, bilirubin levels and oxygen saturation of newborn babies in only 1.25 s by means of self-designed measurement techniques. Ease of use was a key factor in the design, resulting in a device without controls. It relies on a supercapacitor energy buffer, which can be charged wirelessly in less than 5 seconds by touching a Qi charger. Unprecedented wireless through-display powering was studied and applied by placing the Qi receiver coil behind the display. Also an energy study was carried out, revealing that a full buffer provides enough energy for 38 measurements or more than 3 days of standby time. After each measurement, the device automatically transmits the data wirelessly to a computer. The miniaturized device exists of 7 PCBs and contains solely TI ICs (17 pieces). It is equipped with a Qi receiver, a supercap charger, 3 power supplies and a state-of-the-art FRAM microcontroller that controls the sensors, the display, the wireless transmitter and even its own power supplies.

1. Introduction

In present-day hospitals, a lot of handheld diagnostic devices are being used, e.g., thermometers, blood pressure meters, blood glucose meters, pulse oximeters, etc. In general, one device is being used for each kind of measurement. These devices generally have contaminated connectors or battery lids that are difficult to clean and impossible to sterilize. Furthermore, frequent battery replacements decrease ease of use and can cause dangerous situations in case of urgent measurements. Another problem exists in the misplacement of devices, which can result in a loss of time or worse, a neglect to perform measurements when the device cannot be found.

In maternity hospitals, the most frequent measurements performed on babies are temperature measurements, bilirubin measurements and oxygen saturation measurements. Temperature measurements are performed at least daily in the hospital in order to prevent hypothermia and detect signs of infections. Bilirubin measurements are also performed daily, generally by visually checking the yellowness of the baby's skin. These measurements are rather subjective and greatly influenced by lighting conditions. Objective handheld bilirubin meters are available but generally used insufficiently since they use an inefficient xenon lamp, requiring the device to be docked in a charger. High bilirubin levels indicate liver immaturity and can cause brain damage with newborns. Oxygen saturation measurements are performed on 10 percent of the newborns with a mostly bulky, non-portable pulse oximeter in order to detect various vital organ disorders.

In order to solve the previously mentioned problems, a unique diagnostic device for maternity hospitals was invented, the so-called "Tlagnose Watch". This wristband device can be worn by medical staff and is able to measure the three most frequently checked body parameters, being body temperature, bilirubin levels and oxygen saturation. The device is charged wirelessly with a Qi compatible charger in order to prevent hygienic problems (since it can be sealed completely) and increase the comfort of use. A supercapacitor is used for energy storage because this enables charging the device in seconds. This way, the device can effortlessly be charged wirelessly by touching a charging station embedded in the wall. Ease of use is increased even more by leaving out any buttons for controlling the device. One contact with the patient automatically triggers the device to perform all measurements, show the results on the display and transmit them to a central computer. After some time the device automatically turns off. In order to increase device autonomy, an energy efficient circuit was designed.

2. System Architecture

Figure 2 represents a block diagram of the total system. The grey blocks represent the newly designed circuits that together form the watch. All these boards were self-designed and manually developed and assembled. White blocks represent already available hardware that was used in the project, but not self-designed.

From left to right, one can remark the BQ500210EVM evaluation module that is used as a Qi charger. Next, the power supply board implements the Qi receiver, supercapacitor and power circuitry. It is connected to the microcontroller board via an interconnection board that also connects the display. The microcontroller board is also connected to a sensor board for measurements and an RF board for wireless data transmission. This data is transmitted to a TI Launchpad (MSP-EXP430G2) equipped with a CC110L Air boosterpack, that is connected to PC.

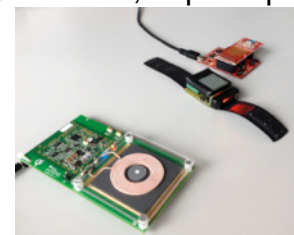


Fig. 1. Total system

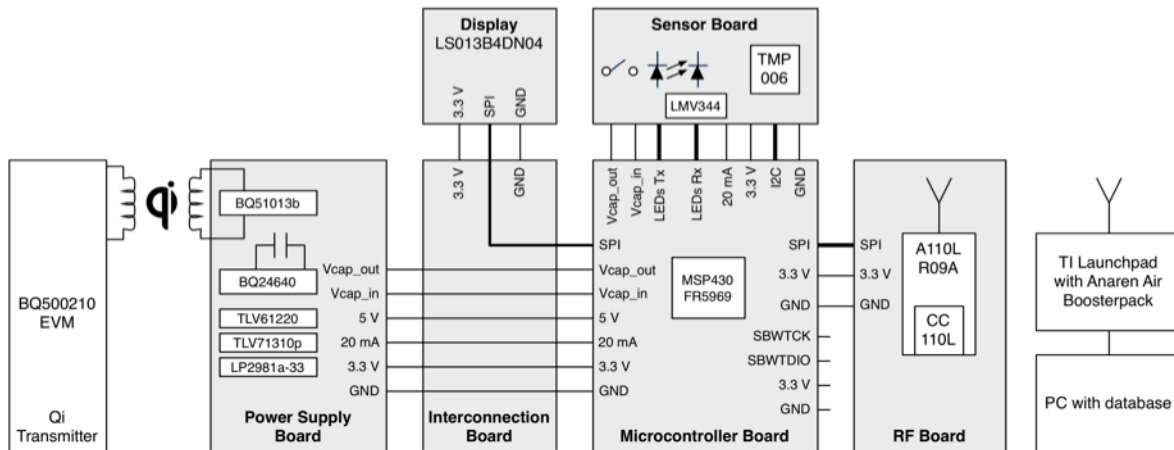


Fig. 2. System architecture

2.1. Power Supply Board

The power supply board contains the Qi-receiver with the Qi receiver coil, the supercap charger with a supercap and three different power supplies. The whole circuit was designed on a single PCB layer so that the bottom layer could be used as a shield for the Qi receiver coil.

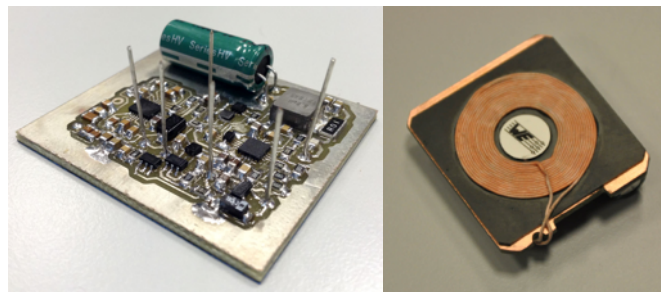


Fig. 3. Power supply board: top and bottom view

2.1.1. Qi Receiver

For the Qi receiver the BQ51013B was selected. This IC is able to provide a stable 5 V, 1 A output and is fully Qi compatible. For the circuit design, the guidelines from the datasheet were followed. As a receiver coil, the 760308201 of Würth Elektronik was chosen for its high quality factor and small size. Because a small form factor is desired for the Tlagnose Watch, the possibility of placing the Qi receiver coil behind the display was investigated. This would imply that wireless power is transmitted through the display. This evaluation was performed for the LS013B4DN04 display from Sharp, which is discussed later. In order to prevent the electromagnetic field from penetrating in the device and its circuits, a copper shield is placed behind the Qi-coil. Figure 4 shows the measurement results of the different configurations, obtained with an Agilent 4285A LCR meter. The Qi receiver in free space clearly has the highest Q-factor and consequently the lowest losses. The copper shield behind the coil increases losses and reduces the Q-factor. When the display is added to the setup, some extra losses are introduced and the Q-factor is reduced further, due to the conducting parts in the display. However the negative influence of adding the display in front of the coil stays very limited,

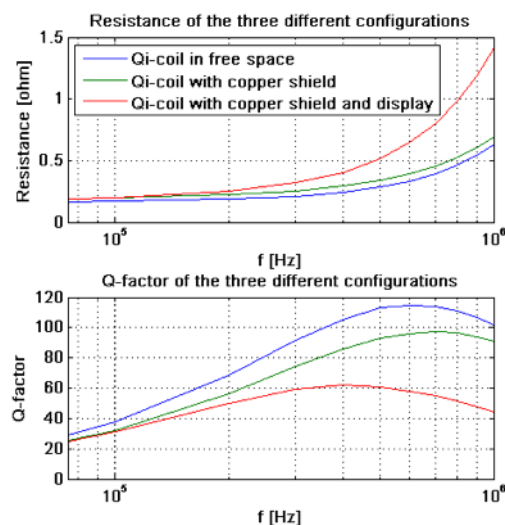


Fig. 4. Qi coil configurations

especially in the 100..205 kHz domain, which is the frequency domain of Qi. At 200 kHz a Q-factor decrease of 68.7 to 50.4 can be observed. This is still high enough to achieve a high power transfer efficiency and to comply with the electrical requirements for Qi receiver coils. Also the mechanical requirements for Qi receivers are met, since the coil is placed within 2.5 mm of the devices outside, given the thin display structure.

2.1.2. Supercap charger

The energy buffer that was used in the Tlagnose Watch is a supercapacitor (HV0820-2R7305-R). It has a capacity of 3 F with a maximal voltage of 2.7 V and is characterized by a very low ESR, enabling very quick charging. A supercap was selected over a rechargeable battery, not only for its charging speed, but also because it has a lifespan of several years with thousands of charge cycles so it never needs replacement. In our application the bq24640 supercap charger IC was selected because its charge current and voltage can be set. By doing so, the maximal current draw from the Qi-receiver IC is limited to 1 A. For the design, the guidelines in the datasheet were followed. Two CSD13202Q2 MOSFETs were selected as switching elements, following these guidelines. However, there are plenty of alternatives (e.g. CSD15571Q2). Figure 5 depicts a comparison between a standard RC circuit with the supercap (current limit 1 A) and our bq24640 charging network. The bq24640 enables charging the supercap in less than 5 seconds, taking the limited power output of the Qi receiver (5 Watts) into account. This is a vast improvement over a standard RC circuit.

A notable disadvantage of supercaps is self-discharging. This phenomenon is visualised for our circuit in Figure 6. After 81 hours the voltage has dropped to 0.55 V, the point where the device stops functioning (since a TLV61220 is used in the power supply). This means that the device has a “standby” time of more than 3 days. This is quite impressive, since only 8 hours (a workers shift) are required.

Also the power draw of the total device was studied. It was found that a complete operation cycle consumes 0.273 J of energy. Given that a charged supercap holds 10.481 J of usable energy (from 2.7 V to 0.55 V), a maximum of 38 measurements can be performed on a single charge. In most of the hospitals, this means that the user only needs to charge the device at the start of the shift, which takes less than 5 seconds.

2.1.3. Power supply outputs

In order to always drive the sensor LEDs (see further) with a stable current of 20 mA, a constant current source was built with the TLV71310p. This linear regulator was chosen for its small form factor and extremely low $V_{in,min}$ of 1.4 V. Given the highest

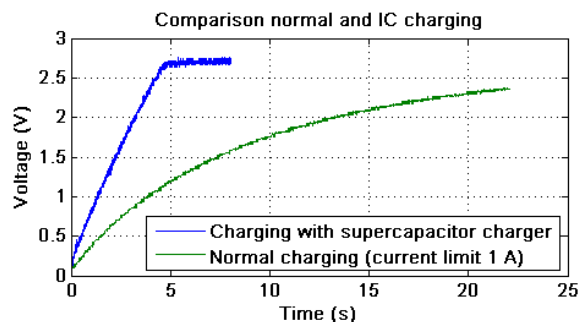


Fig. 5. Charging with RC network or bq24640

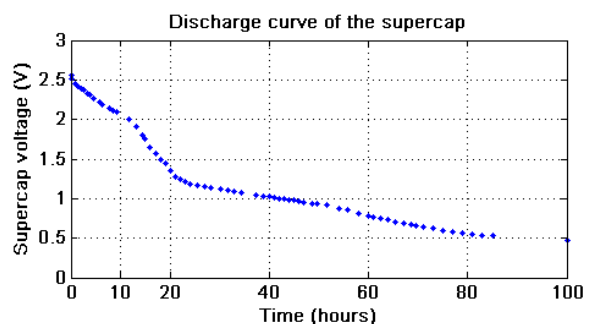


Fig. 6. Discharge curve of the supercap

LED forward voltage of 3.2 V, the minimum input voltage for the current regulator is 4.6 V. Also a take-over contact (see further) is foreseen that needs at least 4.7 V. So it was decided to build a power supply that provides 5 V. Since the supercap has a maximum voltage of 2.7 V that quickly drops, the TLV61220 boost converter was selected for its low $V_{in,min}$ of 0.5 .. 0.7 V, giving access to at least 93 % of the capacitor's energy. The used microcontroller, OPAMPs, TMP006 and CC110L all require a (stable) voltage of 3.3 V. Therefore, the LP2981a-33 was selected for its output current, fast transient response and high accuracy.

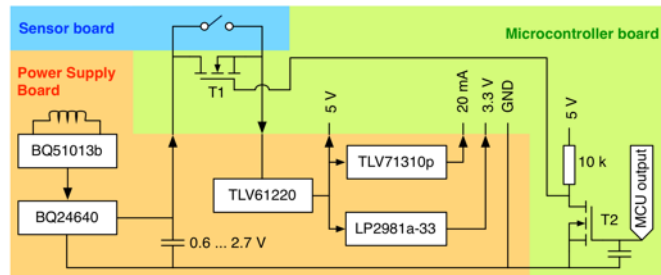


Fig. 7. Power supply block diagram

2.1.1. Take-over contact

Figure 7 depicts a block diagram of the power supplies, including a take-over contact. Initially the switch and MOSFET T1 are open. A push on the switch enables the power supplies, thus the MCU will start. The MCU will keep the gate of MOSFET T2 low. The T1 gate voltage is now 5 V and at least 2.3 V higher than the supercap voltage, so T1 will close. In order to deactivate the system, the MCU puts a high level on the gate of T2. The gate of T1 will be grounded and the MOSFET stops conducting current, decoupling the supercap from the supplies. In order to reactivate the system, the switch needs to be pressed again. This approach avoids any sleep currents, thus maximizing the “standby” time. In this circuit it was important to use the CSD13202Q2 MOSFETs because of their low $R_{DS,on}$ at $V_{GS} = 2.3$ V.

2.2. Sensor Board

The sensor board has 4 important functions to fulfil. Three measurements have to be performed on a patient, being body temperature, bilirubin levels and oxygen saturation of the blood. Also, the device needs to detect when a measurement should be performed. In order to enable all these functions, a reading head was designed and handcrafted in plastic so that all sensors fit in a single casing. This reading head, which is displayed in Figure 8, can be pushed gently against the skin of the newborn to perform all measurements. A tactile switch was integrated in the reading head in order to switch on the device in this occasion (shown in Figure 7). Literature research has indicated that the forehead (or the sternum) is the best place to obtain accurate measurement results for the three body parameters.



Fig. 8. Reading head

2.2.1. Temperature Measurements

For the temperature measurements, several options were considered. It was decided to use an IR thermopile sensor because this enables quick temperature readout without the need to make contact with the patient's skin. The TI TMP006 sensor was selected over (medical grade) sensors such as ZTP-101T from Amphenol Advanced Sensors or MLX90614 from Melexis because of its small size, easy I²C interface, low price, extensive documentation and an urge towards TI components. However, the sensor has an accuracy of $\pm 1^{\circ}\text{C}$, which makes it difficult to obtain accurate body temperature measurements. Furthermore, tests showed that measurements were sometimes disturbed by conduction and convection heat transfers since the sensor

was located too close to the patient's skin. These perturbations could not be solved with mechanical adaptations such as a PE screen between skin and sensor.

So a non-conventional method was elaborated for accurate body temperature measurements with the TMP006 sensor. Since the reading head makes contact with the skin for the bilirubin and oxygen saturation measurements, the temperature can as well be measured by means of a contact measurement. This solution only uses the very precise local die temperature sensor (with a resolution of 0.03125°C) and leaves the thermopile unused. This means that the temperature is measured through heat conduction instead of radiation. An algorithm was elaborated that precisely estimates the body temperature, based on the gradually increasing die temperature when the sensor touches the skin. The basis for this algorithm was a thermal model of the sensor touching the body. The body acts as a heat source for the skin, that on its turn is a heat source for the sensor. Also heat losses to the environment were taken into account. This model can in fact be described as the electrical circuit in Figure 10, given the analogy between voltage and temperature difference, electrical capacity and heat capacity, and electrical resistance and heat resistance. The electrically equivalent circuit was simulated in TINA-TI and Matlab. The results of such a simulation were compared to an experimental dataset in Figure 11, indicating that the model closely matches reality. The mathematical model that resulted from the (Kirchov) analysis of the equivalent circuit, forms the basis of our thermometer operation. It permits predicting the body temperature with an accuracy of 0.15°C in 1.25 seconds, with 5 measurements of the local die temperature. To achieve this accuracy, we assume that the system is calibrated, that constant skin contact is provided during the measurement and that the local die temperature is not more than 20°C lower than the patient's body temperature. However, this last assumption should not be a problem, given that the device is worn on the arm and ambient temperature in a maternity hospital is generally around 20°C .

We can conclude that in spite of the obstacles with using the TMP006 as a body thermometer, acceptable results were achieved, with a non-conventional use of the sensor. The sensor was soldered on a small satellite PCB that fits the reading head and can be mounted on the sensor board, as displayed in Figure 9.



Fig. 9. TMP006

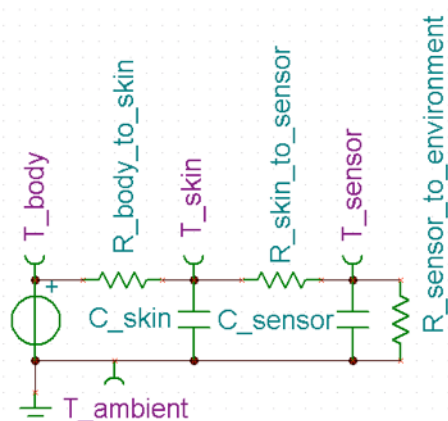


Fig. 10. Temperature model

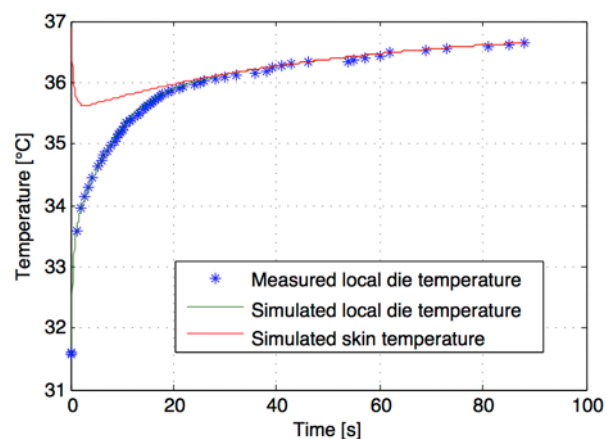


Fig. 11. Simulated temperature model compared to measurements

2.2.2. Bilirubin and Oxygen saturation measurements

Bilirubin, oxyhemoglobin (HbO_2) and deoxygenated hemoglobin (Hb) are blood components that manifest themselves in the skin and subcutaneous tissues. Figure 12 depicts the absorption of light for the most important skin substances. Hb clearly has a higher absorbance than HbO_2 in the 600 to 660 nm region, but HbO_2 has a significantly higher absorbance in the 900 to 1000 nm region. Bilirubin exhibits a peak of absorbance around 450 nm, but around 550 nm, the absorbance is reduced to an insignificant level. It is clear that these optical characteristics form an opportunity for the measurements.

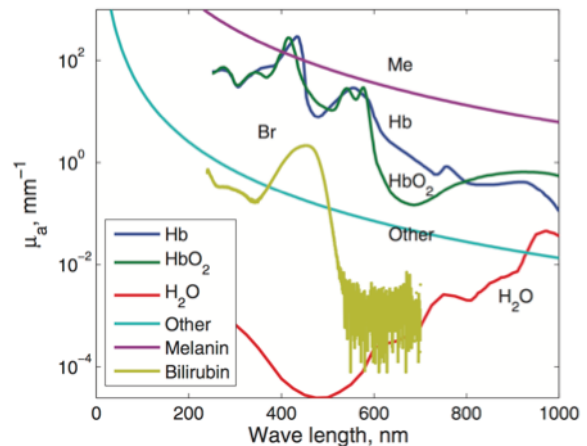


Fig. 12. Coefficients of absorbance

Source: "Reflectance spectrometry of normal and bruised human skins: experiments and modelling", O. Kim et al., 2012

In classic pulse-oximeters, the absorbance of light travelling through a limb is being measured, requiring a light source and receiver on opposite sides of the limb. For our application, a more elegant and user-friendly solution was pursued. Our solution exists of a single reading head that transmits and receives light as depicted in Figure 13. There is no direct path between the light emitter and receiver so the sensor relies on the scattered light in the skin. This implies that a stronger light source and/or a more sensitive receiver are necessary, and a shield between transmitter and receiver should be provided. For the measurements, T1 LEDs from Würth Elektronik and Vishay were used as light emitter (LED) as well as receiver (photodiode):

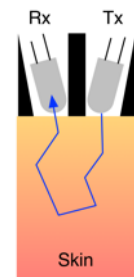


Fig. 13. Optical path

151033(R/G/B)S03000 and TSAL4400. They were selected for their high light output and narrow spectral response at the desired wavelengths of 628 nm (red), 940 nm (infrared), 465 nm (blue) and 525 nm (green). Due to the high light absorbance (especially at short wavelengths), the 4 receiver signals from the photodiodes (current to voltage converted) are too weak for direct connection to a microcontroller's ADC inputs. So 4 OPAMPS are necessary for their high input impedance and an amplification of the signals. The (non-inverting) amplification of the signals increases the resolution of the measurements, since the range of the microcontroller's ADCs can be used optimally. For example, normal measurements resulted in a voltage of 44 mV at the 465 nm photodiode. After amplification, the signal level is boosted to approximately 1 V, leaving room for variation but increasing the resolution of the end result. The LMV344 OPAMP was selected because of its 4 channels, operation at 3.3 V, extremely low input bias current, availability in TSSOP14 package, low supply current, low offset and low price. The TLC274 would be a suitable alternative, but this is a (more expensive) military grade device. Also the AFE4400 was considered but not used in the end because it leaves less room for prototyping, adds hardware that is already available (e.g., ADCs), has a complex QFN40 package, drives only 2 LEDs instead of 4, so two of these ICs would be necessary, and it has a relatively high price point. However, it could be a viable alternative since it reduces the number of components.

The actual measurement of bilirubin and oxygen saturation levels exists in separately flashing each LED and reading the corresponding photodiode output. In order to regulate the intensity of these light flashes, a 20 mA current source was

designed with the TLV71310p, as detailed in the power supply paragraph. The measurements take 1.25 s because this is the minimum time needed for the temperature measurement, and because at least one heartbeat of a newborn will have taken place. In this period, 3 bilirubin measurements and 17 oxygen saturation measurements are performed. Bilirubin levels can be calculated easily since the absorbance of light is linearly correlated to the amount of a substance in the tissue. The bilirubin level is the difference of the blue and green photodiode response, multiplied by a constant and added with another constant. Three measurements are averaged to increase accuracy. Oxygen saturation is determined by subtracting the minimum and the maximum value of the 17 red photodiode responses and doing the same for the infrared responses. The ratio of both subtractions represents the oxygen saturation (via a LUT). Bilirubin and oxygen saturation measurements seemed accurate in early tests, but clinical tests on a significant patient population should be performed in order to evaluate the performance of the measurements and further tune the bilirubin constants and the LUT values.

2.2.3. Sensor board assembly

Figure 14 depicts the design of the sensor board without the plastic reading head. The LMV344 and 2 connectors can be noticed at the back of the PCB. The front is equipped with the TMP006, the LEDs and the switch to start measurements.

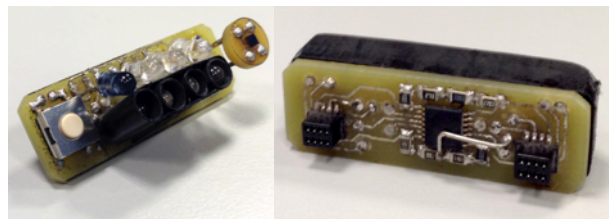


Fig. 14. Sensor board front and backside

2.3. Microcontroller Board

2.3.1. Hardware

A microcontroller was selected for driving the sensors, wireless module and display. These functions require 9 digital outputs, 5 high resolution ADCs, an SPI bus and an I²C bus. The MSP430FR5969 was selected because it meets these requirements with a high number of IO pins and 12-bit ADCs. Furthermore, it is equipped with a large non-volatile memory of 64 kb, operates at a clock frequency of 16 MHz and comes in a compact 48VQFN package. The FRAM technology ensures both high performance and very low power consumption. Recently, several new types that match our requirements were introduced in the FRAM family. Easy prototyping for this project was facilitated by the MSP-BNDL-FR5969LCD.

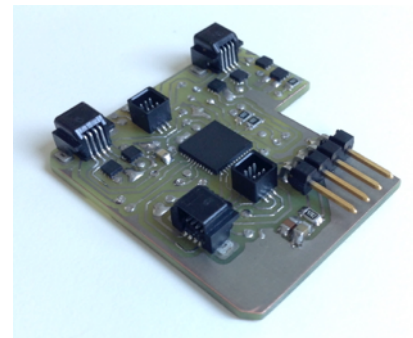


Fig. 15. Microcontroller board

The microcontroller was mounted on a separate central PCB, depicted in Figure 15, with connectors for the interconnection board with its power supply and display signals, the sensor board, the RF board and a Spy-By-Wire interface for programming. Furthermore, 4 MOSFETs were foreseen for switching the 4 LEDs of the sensor board on and off. These MOSFETs were of the CSD13202Q2 type, especially selected for their low $R_{DS(on)}$ at $V_{GS}=3.3$ V, and very small form factor. In terms of I_{DS} capability, these MOSFETs are greatly overdimensioned since I_{DS} for this application is only 20 mA. However, no better match was found in the TI MOSFETs collection, but this is not a problem at all. Also the take-over circuit,

explained in the power supply paragraph, is located close to the microcontroller on this PCB. In this PCB, also a cutout can be remarked, which was foreseen for fitting the supercapacitor in the total assembly in order to reduce the total device thickness. The PCB was designed with all components on one side, in order to facilitate the mounting of the wristband.

2.3.2. Software

In Figure 16, a high level flowchart of the microcontroller software is displayed. When the tactile switch on the sensor board is pressed, the power supplies switch. The microcontroller and the peripherals (the TMP006 via I²C and the display and CC110L via SPI) are then initialized. Next, the pushbutton is bypassed by a take-over contact (MOSFET) controlled by the microcontroller, as explained in the power supply paragraph. This way, the microcontroller stays powered until it deactivates itself. The next steps involve reading the sensors and calculating the body parameters, as explained in the sensor board paragraph. Afterwards, the supercap voltage is measured so that its status can be illustrated with the battery symbol on the display. Subsequently, all the body parameters and supercap status are displayed on the device's screen and the body parameters are transmitted by the CC110L. Then the microcontroller goes into a 10 seconds sleep while the display stays powered, so that the user has enough time for reading the measurement results. When the microcontroller wakes from sleep, it deactivates the take-over contact, cutting its own power and disabling the device completely. The next measurement starts when the tactile switch is pressed again.

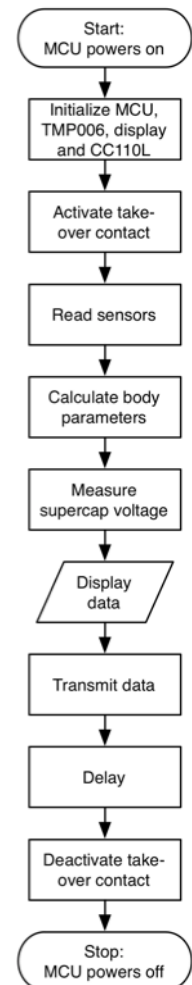


Fig. 16. Flowchart

2.4. Interconnection Board and Display

Since the power supply board was designed on a single PCB layer and the microcontroller board has components mounted on only one side, it was impossible to route connectors for a direct connection between these boards. So an interconnection board was designed to pass through the supply signals and also connect the display to the microcontroller via an SPI interface. It is soldered on the power supply board and plugs onto the microcontroller board.



Fig. 17. Interconnection board

For the display, many options were looked into, ranging from 7-segment, OLED, e-paper and LCD displays. Requirements included operation at 3.3 V, (very) low power usage, dimensions of approximately 1 by 1 inch and detailed controlling documentation. The display that best fits all these requirements is the LS013B4DN04 from Sharp. An extra advantage is that this display is included in the Sharp memory LCD boosterpack, facilitating prototyping. As depicted in Figure 18, the display shows the supercap status and the measured temperature in centigrade, bilirubin levels in mg/dL and oxygen saturation in percent. The display is mounted in front of the Qi coil in a stack of 'Display – Qi Rx coil – copper shield – power supply board – interconnection board'.

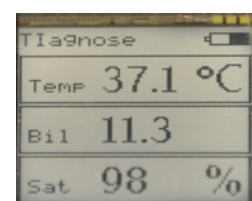


Fig. 18. Display

2.5. RF Board

After calculating the body parameters, they are transmitted to a computer. Therefore, an Anaren A110LR09A (equipped with CC110L) is mounted on a separate board as depicted in Figure 19. This can be plugged onto the microcontroller board. The module was selected for its small form factor, integrated antenna, compliance with both FCC and ETSI standards and easy prototyping with the CC110L Air boosterpack. The CC2540 would be a viable (yet more complex) alternative that also permits direct connection to smartphones and tablets.

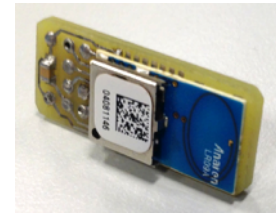


Fig. 19. RF board

The receiver unit consists of a CC110L Air boosterpack (with the same A110LR09A module) on an MSP-EXP430G2 launchpad, which is connected to a PC via USB. The receiver is constantly on, waiting for data packets of a Tlagnose Watch. The watch only acts as a transmitter and broadcasts the body parameters in a single data package of 3 bytes. For the data transmission, the 868.156 MHz carrier is used with 2-FSK modulation and a data rate of 10 kbps. When the data is received by a receiver, it is transferred to a computer via the RS-232 link, as shown in Figure 20.

Also the RSSI is included in this message to the computer. The ultimate goal is to equip every patient's bed with a receiver, so that every measurement can be linked to a patient by processing RSSI data. Experiments showed that this is an achievable goal, but it was not deployed.

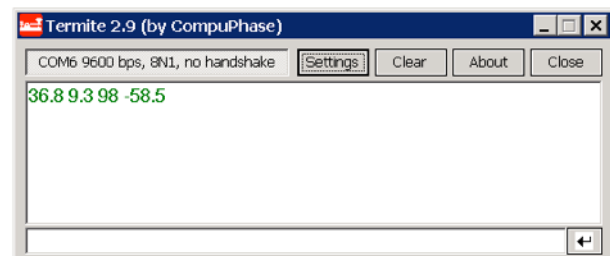


Fig. 20. Received data and RSSI via RS-232

3. Conclusions and Future work

A new type of medical device was designed to perform the 3 most frequent measurements at a maternity hospital, being body temperature, bilirubin levels and oxygen saturation. The device combines emerging technologies like wireless power, supercapacitors, FRAM and memory LCD with established technologies in power supplies, MOSFETs, OPAMPs and wireless communications. The result is an extremely user friendly device that houses 17 TI components in a space of 3.5 x 4 cm and relies on even more TI components in its peripherals.

Future work lies in extensive (clinical) tests and fine tuning the device, as well as expanding the device's functions. Potential improvements in software include heart rate measurement, patient identification with RSSI data or with the optical sensors (when patients are equipped with a colored tag) and 2-way communication so that the PC can send patient information to the Tlagnose Watch. Hardware improvements include further miniaturization with multilayer PCBs, implementing a medical grade thermopile sensor, designing a new blood glucose sensor module for diabetes patients, implementing RFID or NFC patient identification with for example the TMS3705 and BLE support with the CC2540.



Fig. 21. Assembling – charging at wall charger – measuring

Component list Tlagnose Watch					
Device	Value	Qty	Device	Value	Qty
Power supply module			Interconnection board		
Coil	EPL2010-472MLB	1	Capacitor 0805	100n	1
Capacitor 0805	0.1u	4	Connector	IL-WX-6SB-VF	2
Capacitor 0805	1.5n	1	Display connector	XF2L-1025-1	1
Resistor 0805	1M	1	Display	LS013B4DN04	1
Capacitor 0805	1u	7	Microcontroller board		
Resistor 0805	2 Ω	1	Capacitor 0805	100n	2
Tantalum capacitor	3.3u	1	MOSFET	CSD13202Q2	6
Inductor charger	6.8u	1	ISP connector	Pinheader 1X4 90°	1
Resistor 0805	10 Ω	1	Capacitor 0805	2n	1
Resistor 0805	10k	2	Capacitor 0805	1u	1
Sense resistor	10m	1	Resistor 0805	10k	3
Capacitor 0805	10n	2	Resistor 0805	47k	1
Capacitor 0805	10u	6	Connector	IL-WX-6PB-VF	2
Resistor 0805	20k	1	Connector	IL-WX-8PB-HF	3
Capacitor 0805	20u	1	Microcontroller	MSP430FR5969	1
Resistor 0805	22k	1	Sensor board		
Capacitor 0805	22p	1	Resistor 0805	1M	4
Capacitor 0805	33n	1	Resistor 0805	330k	1
Capacitor 0805	47n	3	Resistor 0805	510k	1
Resistor 0805	50 Ω	1	Resistor 0805	30k	1
Capacitor 0805	68n	1	Resistor 0805	220k	2
Resistor 0805	75 Ω	1	Resistor 0805	270k	1
Resistor 0805	100 Ω	1	Resistor 0805	27k	1
Resistor 0805	100k	2	Resistor 0805	430k	1
Capacitor 0805	100n	1	Resistor 0805	750k	1
Resistor 0805	110k	1	Tactile switch	B3FS	1
Resistor 0805	180 Ω	1	Blue LED 3 mm	151033BS0300	2
Resistor 0805	220k	1	Green LED 3 mm	151033GS0300	2
Resistor 0805	220k	1	Connector	IL-WX-8SB-VF	2
Capacitor 0805	220n	2	IR LED 3 mm	TSAL4400	2
Schottky diode	BAT42WS	1	Red LED 3 mm	151033RS0300	2
Supercap charger	BQ24640	1	Quad OPAMP	LMV344	1
Qi receiver IC	BQ51013B	1	Temp sensor	TMP006	1
MOSFET	CSD13202Q2	2	Capacitor 0805	100n	1
LDO voltage reg	LP2981a-33	1	RF board		
Schottky diode	SL13	1	Anaren radio	A110LR09A	1
Supercap	HV0820-2R7305-R	1	Capacitor 0805	100n	1
Step-up convertor	TLV61220	1	Capacitor 0805	10u	1
LDO voltage reg	TLV71310	1	Connector	IL-WX-8SB-VF	1
Qi coil	760308201	1			

IMPORTANT NOTICE

Texas Instruments Incorporated and its subsidiaries (TI) reserve the right to make corrections, enhancements, improvements and other changes to its semiconductor products and services per JESD46, latest issue, and to discontinue any product or service per JESD48, latest issue. Buyers should obtain the latest relevant information before placing orders and should verify that such information is current and complete. All semiconductor products (also referred to herein as "components") are sold subject to TI's terms and conditions of sale supplied at the time of order acknowledgment.

TI warrants performance of its components to the specifications applicable at the time of sale, in accordance with the warranty in TI's terms and conditions of sale of semiconductor products. Testing and other quality control techniques are used to the extent TI deems necessary to support this warranty. Except where mandated by applicable law, testing of all parameters of each component is not necessarily performed.

TI assumes no liability for applications assistance or the design of Buyers' products. Buyers are responsible for their products and applications using TI components. To minimize the risks associated with Buyers' products and applications, Buyers should provide adequate design and operating safeguards.

TI does not warrant or represent that any license, either express or implied, is granted under any patent right, copyright, mask work right, or other intellectual property right relating to any combination, machine, or process in which TI components or services are used. Information published by TI regarding third-party products or services does not constitute a license to use such products or services or a warranty or endorsement thereof. Use of such information may require a license from a third party under the patents or other intellectual property of the third party, or a license from TI under the patents or other intellectual property of TI.

Reproduction of significant portions of TI information in TI data books or data sheets is permissible only if reproduction is without alteration and is accompanied by all associated warranties, conditions, limitations, and notices. TI is not responsible or liable for such altered documentation. Information of third parties may be subject to additional restrictions.

Resale of TI components or services with statements different from or beyond the parameters stated by TI for that component or service voids all express and any implied warranties for the associated TI component or service and is an unfair and deceptive business practice. TI is not responsible or liable for any such statements.

Buyer acknowledges and agrees that it is solely responsible for compliance with all legal, regulatory and safety-related requirements concerning its products, and any use of TI components in its applications, notwithstanding any applications-related information or support that may be provided by TI. Buyer represents and agrees that it has all the necessary expertise to create and implement safeguards which anticipate dangerous consequences of failures, monitor failures and their consequences, lessen the likelihood of failures that might cause harm and take appropriate remedial actions. Buyer will fully indemnify TI and its representatives against any damages arising out of the use of any TI components in safety-critical applications.

In some cases, TI components may be promoted specifically to facilitate safety-related applications. With such components, TI's goal is to help enable customers to design and create their own end-product solutions that meet applicable functional safety standards and requirements. Nonetheless, such components are subject to these terms.

No TI components are authorized for use in FDA Class III (or similar life-critical medical equipment) unless authorized officers of the parties have executed a special agreement specifically governing such use.

Only those TI components which TI has specifically designated as military grade or "enhanced plastic" are designed and intended for use in military/aerospace applications or environments. Buyer acknowledges and agrees that any military or aerospace use of TI components which have **not** been so designated is solely at the Buyer's risk, and that Buyer is solely responsible for compliance with all legal and regulatory requirements in connection with such use.

TI has specifically designated certain components as meeting ISO/TS16949 requirements, mainly for automotive use. In any case of use of non-designated products, TI will not be responsible for any failure to meet ISO/TS16949.

Products

Audio	www.ti.com/audio
Amplifiers	amplifier.ti.com
Data Converters	dataconverter.ti.com
DLP® Products	www.dlp.com
DSP	dsp.ti.com
Clocks and Timers	www.ti.com/clocks
Interface	interface.ti.com
Logic	logic.ti.com
Power Mgmt	power.ti.com
Microcontrollers	microcontroller.ti.com
RFID	www.ti-rfid.com
OMAP Applications Processors	www.ti.com/omap
Wireless Connectivity	www.ti.com/wirelessconnectivity

Applications

Automotive and Transportation	www.ti.com/automotive
Communications and Telecom	www.ti.com/communications
Computers and Peripherals	www.ti.com/computers
Consumer Electronics	www.ti.com/consumer-apps
Energy and Lighting	www.ti.com/energy
Industrial	www.ti.com/industrial
Medical	www.ti.com/medical
Security	www.ti.com/security
Space, Avionics and Defense	www.ti.com/space-avionics-defense
Video and Imaging	www.ti.com/video

TI E2E Community

e2e.ti.com